SEMARAK ILMU PUBLISHING

Semarak International Journal of Nanotechnology

Journal homepage:
https://semarakilmu.com.my/journals/index.php/sijn/index

Mxene and Strontium Titanate Hybrid Casson Nanofluid with CMC Base *via* the Caputo-Fabrizio Fractional Derivative over a Vertical Riga Plate

Ridhwan Reyaz[1], Ahmad Qushairi Mohamad[1,*], Yeou Jiann Lim[1], Arshad Khan[2], Sharidan Shafie[1]

[1] Department of Mathematical Sciences, Faculty of Science, Universiti Teknologi Malaysia, Skudai, Johor Bahru, 81310, Johor, Malaysia
[2] Institute of Computer Sciences and Information Technology (ICS/IT), The University of Agriculture, Peshawar, 25130 Khyber Pakhtunkhwa, Pakistan

ARTICLE INFO

Article history:
Received : 21 March 2024
Received in revised form : 15 April 2024
Accepted : 5 May 2024
Available online : 10 June 2024

Keywords:
Mxene; Strontium Titanate; hybrid nanofluid; Caputo-Fabrizo fractional derivative; Riga plate; Laplace transform

ABSTRACT

Mxene nanoparticles possess desirable properties such as high electrical conductivity, aqueous stability, and thermal stability, making them highly sought-after in various fields including manufacturing, renewable energy, and chemical engineering. Similarly, Strontium Titanate ($SrTiO_3$) is a versatile material with high electrical conductivity and low thermal expansion properties, applicable in electronics, solar energy, and biomedical engineering. This study aims to investigate the effects of a hybrid nanofluid consisting of Mxene and Strontium Titanate in a Carboxymethyl Cellulose (CMC) base, using the Caputo-Fabrizio fractional derivative, over a Riga plate. The fractional derivative is a concept with future applications, while Riga plates act as actuators for fluid flow in marine vessels. Laplace transform is used to find solutions from the governing PDEs, analytically. The resulting integral solution is analysed graphically and numerically. According to the study, a rise in the fractional parameter, α, causes an increase in fluid temperature and velocity. Because of the unique features of $SrTiO_3$, the thermal radiation parameter N has a distinct effect on velocity and temperature. As N increases, the temperature rises but velocity declines. Due to the high electrical conductivity of Mxene and $SrTiO_3$, the modified Hartmann number, E, favourably influences velocity. Skin friction increases due to $SrTiO_3$ whereas the Nusselt number falls with increasing N due to CMC base characteristics.

1. Introduction

Fluids are commonly used to transfer heat from one medium to another. Applications of heat transfer for fluid can be seen everywhere, including in electrical devices such as refrigerators, computers and air conditioning all the way to nuclear power plants to regulate heat in the thermal reactors. The invention of nanofluids greatly enhanced the properties of heat transfer in fluids. Early in the 1990s, scientists made the discovery that adding nanoparticles to a fluid accelerates the rate of heat transmission. This was made by Choi and Eastman [1]. Water, ethylene glycol, oil, copper, aluminium, ferromagnesium and oxide metals are the typical fluid bases and nanoparticles utilized

* *Corresponding Author.*
E-mail address: ahmadqushairi@utm.my

in nanofluids. Numerous investigations have been conducted on the boundary layer flow of nanofluids. For instance, Khalid *et al*., [2] conducted an analytical investigation on the free convection flow of nanofluid with ramped wall effect. The study looked at how five distinct kinds of nanoparticles behaved in a fluid with a water basis and solved the PDE system using the Laplace transform. To clarify the nanofluid's temperature and velocity patterns, analytical solutions were obtained. Aly and Ebaid [3], on the other hand, conducted an analytical analysis on the rate of heat transfer for nanofluids with magnetohydrodynamic (MHD) and Marangoni radiation effects. Using water base nanofluids with MHD and radiation absorption effects, Durga *et al*., [4] conducted an analytical investigation for heat and mass transfer for Copper and Titanium Oxide. Other analytical and numerical investigations on nanofluids were done by Hussanan *et al.,* [5], Souayeh *et al.,* [6], Uddin and Rasel [7], Mahanta *et al*., [8], Veera and Chamkha [9], Aleem *et al*., [10] and Anwar *et al.,* [11]. In the search for improving heat transfer rates within nanofluids, the search for new and ideal nanoparticles and base fluid is still at its peak. Recently, new nanoparticles that were just discovered during the past few years are Mxene and Strontium Titanate ($SrTiO_3$). Also, a new base fluid that is uncommon for nanofluids is the Carboxymethyl Cellulose (CMC) fluid.

A new substance called Mxene has received a lot of attention lately. It is made of carbon-nitrides, nitrides, and carbides in 2D [12,13]. Mxenes have many desirable properties that are worth investigating. They have a high surface area, providing a huge platform for chemical reactions, they are excellent electrical conductors and are very stable in an aqueous environment, making them very suitable for nanofluids. Mxenes also have good biocompatibility, opening them up for multiple applications in the biomedical engineering field [14-16]. Meanwhile, Strontium Titanate nanoparticles are transparent materials with high electrical conductivity properties. They are a type of perovskite oxide material [17-19]. The properties of $SrTiO_3$ make it highly sought after in the optical industry. There is rarely any research on flow across the boundary layer for nanofluids including Mxene or $SrTiO_3$ nanoparticles. Thus, the effect of these nanoparticles on fluid flow within a boundary layer is worth investigating. Furthermore, to elevate the effectiveness of nanofluids, hybrid nanofluid is also worth considering. It is observed from published studies that hybrid nanofluids offer a higher rate of thermal conductivity at the same time, reducing the cost of materials [20-24].

In contrast, CMC is an instance of a water-soluble polymer that is a non-Newtonian fluid. It is often used as a thickening agent for the food and cosmetic industry [25]. According to experimental studies, one of the mathematical model that is suitable to model the fluid flow of CMC fluids is the Casson fluid model [26,27]. There are a few studies on boundary layer flow for CMC based nanofluids using the Casson model. Using CMC as the basis of the fluid, Alwawi *et al*., [28] performed a numerical investigation on a mixed convection Casson nanofluid from a spherical. Meanwhile, Ali *et al*., [29] investigated the irreversibility analysis of cross fluid with Copper Oxide-Titanium Oxide hybrid nanofluid with CMC base. The behaviour of CMC-based Casson nanofluid flowing across a stretched plate is examined in another work for CMC-based Casson nanofluid by Rawi *et al*., [30]. These research employ numerical techniques to solve the underlying partial differential equations. Saqib *et al.,* [31,32] conducted analytical research on CMC-based nanofluids. It is pertinent to point out that Saqib *et al*., [31,32] also looked at how partial derivatives affect how fluid flows in the boundary layer.

Fractional derivatives are perceptions where the conventional derivative is considered to have an order of an arbitrary number or fraction. Factional derivatives have been defined in a number of ways since they were first introduced, including the Riemann-Liouville, Hilfer, Caputo, Caputo-Fabrizio, Atangana-Baleanu, and many others [33-35]. Due to its non-singular kernel quality, the CaputoFabrizio fractional derivative (CFFD) is one of the most favoured definitions. In contrast to Caputo and Atangana-Baleanu derivatives, the CFFD solution of a PDE yields an integral function devoid of any special functions. Fractional derivatives are not yet represented geometrically or

physically in the realm of fluid mechanics. But the literature claims that when the fractional derivative is taken into account in the fluid mechanics model, a different but workable solution is produced. Researchers will likely employ these technologies to validate their findings in the near future. In order to study the behaviour of a fluid flow, fractional derivatives are therefore significant enough. The flow of boundary layers with fractional derivatives has been the subject of various investigations over the years. Khan *et al.,* [36] pioneered the study of analytical solutions of boundary layer flow with fractional derivative by considering the Caputo derivative. The Caputo derivative, however, is known to have unique kernels. As a result, analytical solutions in the shape of unique functions, like the Wright and Mittag-Lefler functions, are obtained. Abro and Khan use Abro [37] for analyzing the impact of carbon nanotubes (CNTs) on methanol-based nanofluids flowing across a vertical plate. The fractional derivative was taken into account, specifically the Caputo-Fabrizio definition. From their investigations, it is observed that there are no specific functions in the final analytical solutions. Other research on fractional derivatives and the Caputo-Fabrizio fractional derivative can be found in the works of Maiti *et al*., [38], Raza and Ullah [39], Reyaz *et al*., [40], and Sene [41]. Reyaz *et al*., recently investigated the laminar flow of a Casson fluid [42]. In addition to considering a fractional derivative model, they also considered the fluid to be moving along a Riga plate in an upright position. It is also worth mentioning that the definition for the fractional derivative that the considered was the Caputo-Fabrizio definition.

Riga plates are flat plates with electrodes and magnets arranged in alternating order. It is often used as an actuator to control fluid flow and reduce turbulence. Primarily, it is often used in the marine engineering field for submarines and aquatic vessels. The presence of electrodes and magnets induces an electromagnetic current which in turn produces an upthrust force, often referred to as the Lorentz force. The resultant Lorentz force can be employed to facilitate or obstruct fluid flow, depending on where the Riga plate is located. An analytical investigation was conducted by Asogwa *et al*., [43] on the presence of a Riga plate on a double convection fluid flow. Similarly, the fluid considered was a Casson fluid. It is also worth noting that the presence of a Riga plate is analyzed mathematically by the value of the Lorentz force it generates. Asogwa *et al*., [44] conducted comparative analytical research on water-based nanofluids made of alumina-oxide and copper-oxide that were flowing vertically across a Riga plate. The Riga plate is found to stimulate fluid flow, and copper oxide performs better overall as a thermal conductor than alumina oxide. Khatun *et al*., [45] did a similar study with similar results. Other studies on the Riga plate to note include Mallawi *et al*., [46], Campus and Africa [47], Bilal *et al.*, [48], Logantahan and Deepa [49] and Nasrin *et al*., [50].

As per the information available currently, no analytical study of the behaviour of fluid flow for the boundary layer with Mxene $SrTiO_3$ hybrid Casson nanofluid with CMC base *via* the CaputoFabrizio fractional derivative over a moving vertical Riga plate has been carried out. The purpose of this study is to close this gap by analyzing the impacts of parameter modification on fluid velocity and temperature and providing an analytical solution using the Laplace transform.

2. Mathematical Formulation

Consideration is being given to the flow of a Casson hybrid nanofluid over an infinitely accelerated Riga plate under the influence of free convection. The Riga plate is positioned vertically along the x -axis with the y -axis being perpendicular to it. Movement of the nanofluid is in the same direction as the x -axis when $y > 0$. Initially, the Riga plate is stationary and the ambient temperature is Θ_∞ at time $\tau = 0$. Subsequently, the Riga plate starts moving at a speed of v_0 and maintains a temperature of Θ_W as time progresses. The motion of the Riga plate induces an electromagnetic field, leading to

the generation of the Lorentz force, F, which acts as an upward force in the x-direction. Additionally, thermal radiation, q_r, perpendicular to the x-axis, uniformly penetrates the system. It is assumed that the Reynolds number is relatively low, resulting in the negligible impact of the magnetic field generated by the fluid motion. The relationship between the velocity, v, and the temperature, Θ, is determined by the variables y and τ. The fluid flow and the structure of the Riga plate are visualized in Figure 1 and 2, respectively.

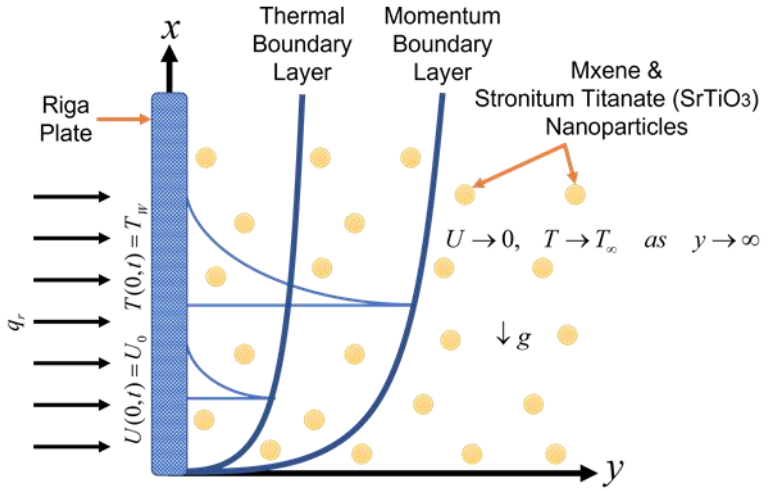

Fig. 1. Geometrical representation of fluid flow

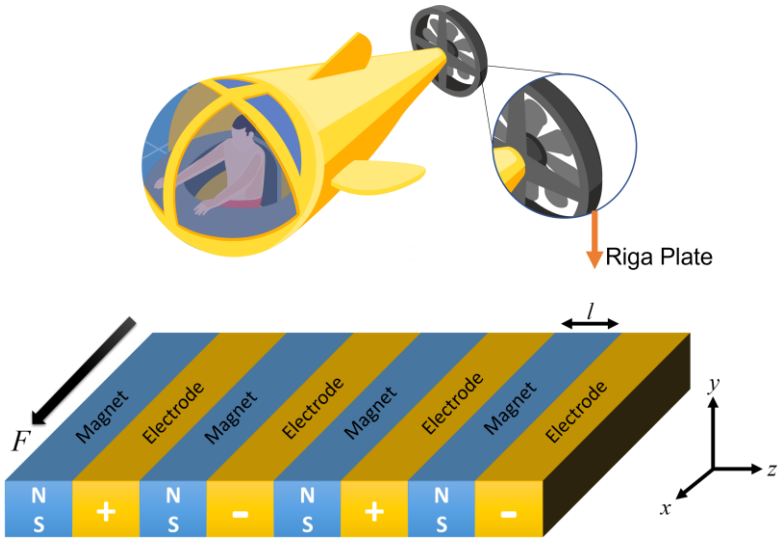

Fig. 2. A Riga plate and its application

The following governing momentum and energy equations are obtained using Boussinesq's approximation and the aforementioned assumptions [51, 52, 53, 42]:

$$\frac{\partial v(y,\tau)}{\partial \tau}=\frac{\mu_{hnf}}{\rho_{hnf}}\left(1+\frac{1}{\gamma}\right)\frac{\partial^2 v(y,\tau)}{\partial y^2}+\frac{(\rho\beta_T)_{hnf}\,g}{\rho_{hnf}}(\Theta-\Theta_\infty)+\frac{\pi J_0 M_0}{8\rho_{hnf}}\exp\left(-\frac{\pi}{l}y\right), \tag{1}$$

$$(\rho C_P)_{hnf}\frac{\partial \Theta(y,\tau)}{\partial \tau}=k_{hnf}\frac{\partial^2 \Theta(y,\tau)}{\partial y^2}-\frac{\partial q_r}{\partial y}. \tag{2}$$

Eq. (1) and (2) are both constrained by conditions:

$$\begin{aligned} &\nu(y,0)=0, \quad \nu(0,\tau)=U_0, \quad \nu(\infty,\tau)\to 0, \\ &\Theta(y,0)=\Theta_\infty, \quad \Theta(0,\tau)=\Theta_W, \quad \Theta(\infty,\tau)\to 0. \end{aligned} \tag{3}$$

In our analysis, the dynamic viscosity is represented by μ, the fluid density by ρ, the Casson fluid parameter by γ, the thermal expansion coefficient by β_T, the gravitational acceleration by g, the electrical current density by J_0, the magnetization strength by M_0, and the width of the magnets and electrodes by l. The specific heat capacity of the fluid at constant density is denoted as C_P. Furthermore, we use the symbols q_r to denote the thermal radiation value and k for the thermal conductivity parameter. Rosseland's approximation, cited by [54, 55, 56], reduces the governing energy equation from Eq. (2) to:

$$\left(\rho C_P\right)_{hnf}\frac{\partial\Theta(y,\tau)}{\partial\tau}=k_{hnf}\frac{\partial^2\Theta(y,\tau)}{\partial y^2}+\frac{16\sigma_1 T_\infty^3}{3k_1}\frac{\partial^2\Theta(y,\tau)}{\partial y^2}. \tag{4}$$

The mean absorption coefficient is represented by k_1, while the Stefan-Boltzmann constant is denoted as σ_1. Notably, the physical properties of the hybrid nanofluid are symbolized by the subscript hnf. As per the Tiwari and Das model [57, 58, 59], the thermophysical properties of the base fluid and nanoparticles are detailed in Table 1.

Table 1
Thermophysical properties of base fluid and nanoparticles

	$\rho\,(kg/m^3)$	$C_P\,(J/kg\cdot K)$	$k\,(W/m\cdot K)$	$\beta_T\,(K^{-1})$	Pr
Carboxymethyl Cellulose (CMC)	997.2	4179	0.613	$21\cdot 10^{-5}$	6.2
Mxene	4000	650	350	$8.3\cdot 10^{-6}$	-
Strontium Titanate ($SrTiO_3$)	5120	540	12	$10.4\cdot 10^{-6}$	-

$$\mu_{hnf}=\frac{\mu_f}{(1-\phi_1)^{2.5}(1-\phi_2)^{2.5}}, \tag{5}$$

$$\rho_{hnf}=(1-\phi_2)\left[(1-\phi_1)\rho_f+\phi_1\rho_{s1}\right]+\phi_2\rho_{s2}, \tag{6}$$

$$(\rho\beta_T)_{hnf}=(1-\phi_2)\left[(1-\phi_1)(\rho\beta_T)_f+\phi_1(\rho\beta_T)_{s1}\right]+\phi_2(\rho\beta_T)_{s2}, \tag{7}$$

$$(\rho C_P)_{hnf}=(1-\phi_2)\left[(1-\phi_1)(\rho C_P)_f+\phi_1(\rho C_P)_{s1}\right]+\phi_2(\rho C_P)_{s2}, \tag{8}$$

$$k_{bf}=k_f\left[\frac{(k_{s_1}+2k_f)-2\phi_1(k_f-k_{s_1})}{(k_{s_1}+2k_f)+\phi_1(k_f-k_{s_1})}\right], \tag{9}$$

$$k_{hnf} = k_{bf}\left[\frac{(k_{s_2} + 2k_{bf}) - 2\phi_2(k_{bf} - k_{s_2})}{(k_{s_2} + 2k_{bf}) + \phi_1(k_{bf} - k_{s_2})}\right], \tag{10}$$

where, φ is the nanoparticle volume fraction and ϕ_1 and ϕ_2 are the nanoparticle volume fractions of Mxene and Strontium Titanate ($SrTiO_3$) particles, respectively. The attributes for base fluid and nanoparticle, respectively, are represented by the subscripts f and s. The kinematic viscosity, fluid density, thermal expansion, specific heat capacity, base fluid thermal conductivity, and hybrid nanofluid thermal conductivity equations range from Eq. (5) to (10). Eq. (1) and (4) must be solved with a set of dimensionless parameters, as illustrated in the following Eq. (11).

$$U^* = \frac{U}{U_0}, \quad y^* = y\frac{U_0}{\upsilon}, \quad \tau^* = \tau\frac{U_0^2}{\upsilon}, \quad \Theta^* = \frac{\Theta - \Theta_\infty}{\Theta_W - \Theta_\infty}. \tag{11}$$

Utilizing definitions of thermophysical properties for nanofluid and base fluid from Eq. (5) to (10) as well as the dimensionless parameters from Eq. (11) [5,60,61]. Eq. (1), (3) and (4) are further reduced to their dimensionless form as follows by eliminating the asterisk (*) notation:

$$\frac{\partial \nu(y,\tau)}{\partial \tau} = \frac{\varphi_3}{\varphi_4}\gamma_0\frac{\partial^2 \nu(y,\tau)}{\partial y^2} + \frac{\varphi_5}{\varphi_4}GrT(y,\tau) + \frac{1}{\varphi_4}E\exp(-Ly), \tag{12}$$

$$\frac{\partial \Theta(y,\tau)}{\partial \tau} = \left(\frac{\varphi_2}{\varphi_1} + \frac{4}{3\varphi_1}N\right)\frac{1}{\Pr}\frac{\partial^2 \Theta(y,\tau)}{\partial y^2}, \tag{13}$$

bounded by dimensionless initial and boundary conditions:

$$\begin{aligned} &\nu(y,0) = 0, \quad \nu(0,\tau) = 1, \quad \nu(\infty,\tau) \to 0, \\ &\Theta(y,0) = 0, \quad \Theta(0,\tau) = 1, \quad \Theta(\infty,\tau) \to 0, \end{aligned} \tag{14}$$

where γ_0, Gr, E, L, N, $\Pr$ and ϕ_n for $n = 1, 2, \ldots, 5$ are defined as:

$$\begin{aligned} &\gamma_0 = 1 + \frac{1}{\gamma}, \qquad Gr = \frac{\upsilon g\beta_T(\Theta_W - T_\infty)}{U_0^{\,3}}, \quad E = \frac{\pi J_0 M_0 \upsilon}{U_0^{\,3} 8\rho}, \quad L = \frac{\pi\upsilon}{lU_0}, \quad N = \frac{4\sigma_1 T_\infty^3}{k_1 k_f}, \\ &\Pr = \frac{\upsilon(\rho C_P)_{hnf}}{k_{hnf}}, \quad \varphi_1 = \frac{(\rho C_P)_{hnf}}{(\rho C_P)_f}, \qquad \varphi_2 = \frac{k_{hnf}}{k_f}, \qquad \varphi_3 = \frac{\mu_f}{\mu_{hnf}}, \quad \varphi_4 = \frac{\rho_{hnf}}{\rho_f}, \\ &\varphi_5 = \frac{(\rho\beta_T)_{hnf}}{(\rho\beta_T)_f}. \end{aligned} \tag{15}$$

Here, the dimensionless Casson fluid parameter is denoted by γ_0, the Grashof number by Gr, the modified Hartmann number by E, the dimensionless constant parameter by L, the

dimensionless thermal radiation parameter by N, the Prandtl number by Pr, and the dimensionless nanoparticle volume fraction parameter by ϕ_n for $n = 1, 2, ..., 5$.

$$D_t^{\alpha} f(y,\tau) = \frac{1}{1-\alpha}\int_0^{\tau} \frac{\partial f(y,s)}{\partial y} exp\left(-\alpha \frac{\tau - s}{1-\alpha}\right) ds, \tag{16}$$

$$\mathrm{L}\{D_t^{\alpha} f(y,\tau)\} = \frac{q\bar{f}(y,q) - f(y,0)}{q + \alpha(1-q)}. \tag{17}$$

The equations for the Caputo-Fabrizio fractional derivative Eq. (16) and its corresponding Laplace transforms Eq. (17) provide the definitions. In these expressions, the Laplace transform, L, the frequency domain, q, and the fractional derivative parameter, α, are utilized. The fractional derivative, $D_t^{\alpha}(\cdot)$, from Eq. (16) is substituted with the partial derivative with respect to time, $\frac{\partial}{\partial \tau}$, in Eq. (12) and (13), transforming them into fractional governing momentum and energy equations, respectively.

$$D_t^{\alpha} v(y,\tau) = \frac{\varphi_3}{\varphi_4}\gamma_0 \frac{\partial^2 v(y,\tau)}{\partial y^2} + \frac{\varphi_5}{\varphi_4} GrT(y,\tau) + \frac{1}{\varphi_4} E \exp(-Ly), \tag{18}$$

$$D_t^{\alpha} \Theta(y,\tau) = \left(\frac{\varphi_2}{\varphi_1} + \frac{4}{3\varphi_1} N\right) \frac{1}{\mathrm{Pr}} \frac{\partial^2 \Theta(y,\tau)}{\partial y^2}, \tag{19}$$

3. Mathematical Formulation

The governing equations Eq. (18) and Eq. (19) were first reduced to a frequency domain, q, using the Laplace transform before being used to obtain the final analytical solutions. The momentum and energy equations' answers are written down using the method of Laplace transform as follows:

$$\begin{aligned} \bar{U}(y,q) = {} & \left[\frac{1}{q} + \frac{Gr_1}{a_0}\left(\frac{q+a_1}{q^2}\right) + E_0\left(\frac{q+a_1}{q^2 C_2 + qC_3)}\right)\right] \exp\left(-y\sqrt{\frac{1}{B_1}}\sqrt{\frac{a_0 q}{q+a_1}}\right) \\ & - \frac{Gr_1}{a_0}\frac{q+a_1}{q^2}\exp\left(\sqrt{\frac{a_0}{\mathrm{Pr}_1}}\sqrt{\frac{q}{q+a_1}}\right) - E_0\left(\frac{q+a_1}{q^2 C_2 + qC_3}\right)\exp(-Ly), \end{aligned} \tag{20}$$

$$\bar{\Theta}(y,q) = \frac{1}{q}\exp\left(-y\sqrt{\frac{a_0}{\mathrm{Pr}_1}}\sqrt{\frac{q}{q+a_1}}\right). \tag{21}$$

The constant parameters Gr_1, a_0, a_1, E_0, B_0, C_2, C_3 and Pr_1 are expressed as:

$$Gr_1 = \frac{Gr_0}{C_1 B_1} \quad Gr_0 = \frac{\varphi_5}{\varphi_4} Gr, \quad C_1 = \frac{1}{Pr_1} - \frac{1}{B_1}, \quad B_1 = \frac{\varphi_3}{\varphi_4}\gamma_0, \quad a_0 = \frac{1}{1-\alpha},$$
$$a_1 = \alpha a_0, \quad E_0 = \frac{1}{\varphi_4} E, \quad C_2 = B_1 L^2 - a_0, \quad C_3 = B_1 L^2 a_1, \quad \mathrm{Pr}_1 = \left[\frac{\varphi_4}{\varphi_5} + \frac{4}{3}\frac{N}{\varphi_5}\right]^{-1} \mathrm{Pr}. \tag{22}$$

Next, Eq. (20) and (21) are separated into:

$$\bar{\xi}_1(y,q) = \frac{1}{q^2} + \bar{\xi}_2(y,q) + \bar{\xi}_3(y,q), \quad \bar{\xi}_2(y,q) = -\frac{Gr_1}{a_0}\frac{q+a_1}{q^2},$$
$$\bar{\xi}_3(y,q) = -E_0 \frac{q+a_1}{q^2 C_2 + qC_3}, \qquad \bar{\xi}_4(y,q) = \frac{1}{q}, \tag{23}$$

and

$$\bar{\psi}_1(y,q) = \exp\left(-y\sqrt{\frac{a_0}{B_1}}\sqrt{\frac{q}{q+a_1}}\right), \quad \bar{\psi}_2(y,q) = \exp\left(-y\sqrt{\frac{a_0}{\mathrm{Pr}_1}}\sqrt{\frac{q}{q+a_1}}\right). \tag{24}$$

Indicating an inverse Laplace transform product, such as:

$$\mathrm{L}^{-1}\{\bar{\xi}_1(y,q)\} = \xi_1(y,\tau), \quad \mathrm{L}^{-1}\{\bar{\xi}_2(y,q)\} = \xi_2(y,\tau), \quad \mathrm{L}^{-1}\{\bar{\xi}_3(y,q)\} = \xi_3(y,\tau),$$
$$\mathrm{L}^{-1}\{\bar{\xi}_4(y,q)\} = \xi_4(y,\tau), \quad \mathrm{L}^{-1}\{\bar{\psi}_1(y,q)\} = \psi_1(y,\tau), \quad \mathrm{L}^{-1}\{\bar{\psi}_2(y,q)\} = \psi_2(y,\tau), \tag{25}$$

where, L^{-1} is the inverse Laplace transform notation. Eq. (23)'s inverse Laplace transform is written as:

$$\xi_1(y,\tau) = 1 + \xi_2(y,\tau) + \xi_3(y,\tau), \qquad \xi_2(y,\tau) = -\frac{Gr_1}{a_0}(1 + a_1 t),$$
$$\xi_3(y,\tau) = -\frac{E_0}{C_2 C_3}\left[a_1 C_2 + \left(C_3 - a_1 C_2\right)\exp\left(-\frac{C_3}{C_2}\tau\right)\right], \quad \xi_4(y,\tau) = 1. \tag{26}$$

In the meanwhile, the compound function of the inverse Laplace transform approach was used to generate the inverse Laplace transform of Eq. (24) [62-64]:

$$\psi_1(y,\tau) = \int_0^\infty \frac{\sqrt{a_0/B_1}}{2\sqrt{\pi}u^{3/2}} \exp\left(-\frac{a_0/B_1}{4u} - uy^2 - a_1 t\right)\left[\sqrt{\frac{a_1 y^2}{\tau}}\mathrm{I}_1\left(2\sqrt{a_1 y^2 t}\right) + \delta(\tau)\right] du,$$
$$\psi_2(y,\tau) = \int_0^\infty \frac{\sqrt{a_0/\mathrm{Pr}_1}}{2\sqrt{\pi}u^{3/2}} \exp\left(-\frac{a_0/\mathrm{Pr}_1}{4u} - uy^2 - a_1 t\right)\left[\sqrt{\frac{a_1 y^2}{\tau}}\mathrm{I}_1\left(2\sqrt{a_1 y^2 t}\right) + \delta(\tau)\right] du. \tag{27}$$

The modified Bessel function of the first kind of order one and the Dirac delta function are represented by the notations $I_1(\cdot)$ and $\delta(\cdot)$, respectively. The solutions to Eq. (20) and (21) are

denoted by $\nu(y,\tau)$ and $\Theta(y,\tau)$, and after an inverse Laplace transformation, they are expressed as the convolution product in the following manner:

$$\nu(y,\tau)=\int_0^\tau \xi_1(y,\tau-s)\psi_1(y,s)ds+\int_0^\tau \xi_2(y,\tau-s)\psi_2(y,s)ds+\xi_3(y,\tau)\exp\left(-Ly\right), \tag{28}$$

The final analytical solutions of the momentum and energy equations, as per Eq. (28) and (29), can be obtained by substituting Eq. (26) and (27), and replacing the modified Bessel function with its integral form in Eq. (20) and (21).

$$\begin{aligned}\nu(y,\tau)=&\int_0^\infty \frac{E_0}{a_0C_2C_3}\exp\left(-\frac{C_3}{C_2}\tau\right)\left[a_0(C_3-a_1C_2)\exp\left(\frac{C_3}{C_2}\tau\right)\left(a_0(a_1C_2+C_1C_3)+C_1C_3Gr_1(1+a_1t)\right)\right]\\
&\frac{\sqrt{a_0/B_1}}{2\sqrt{\pi}u^{3/2}}\left[2\Phi(\tau)-1\right]\exp\left(-\frac{a_0/B_1}{4u}-uy^2\right)du\\
&+\int_0^\infty\int_0^\tau\int_0^\pi \frac{1}{\pi}\frac{\sqrt{a_0/B_1}}{2\sqrt{\pi}u^{3/2}}\sqrt{\frac{a_1uy^2}{s}}\cos(\theta)\left[(\tau-s)-\frac{Gr_1}{a_0}\left(1+a_1(\tau-s)\right)\right.\\
&\left.-\frac{E_0}{C_2C_3}\left(a_1C_2+(C3-a_1C_2)\exp\left(-\frac{C_3}{C_2}(\tau-s)\right)\right)\right]\\
&\exp\left(-\frac{a_0/B_1}{4u}-uy^2-a_1s+(2\sqrt{a_1uy^2s})\cos(\theta)\right)d\theta dsdu\\
&-\int_0^\infty \frac{Gr_1}{a_0}\frac{\sqrt{a_0/\mathrm{Pr}_1}}{2\sqrt{\pi}u^{3/2}}\exp\left(-\frac{a_0/\mathrm{Pr}_1}{4u}-uy^2\right)(a_1t+1)\left[2\Phi(\tau)-1\right]du\\
&-\int_0^\infty\int_0^\tau\int_0^\infty \frac{1}{\pi}\frac{Gr_1}{a_0}\frac{\sqrt{a_0/\mathrm{Pr}_1}}{2\sqrt{\pi}u^{3/2}}\sqrt{\frac{a_1uy^2}{s}}\left(1+a_1(\tau-s)\right)\cos(\theta)\\
&\exp\left(-\frac{a_0/\mathrm{Pr}_1}{4u}-uy^2-a_1s+(2\sqrt{a_1uy^2s})\cos(\theta)\right)d\theta dsdu\\
&-\frac{E_0}{C_2C_3}\left[a_1C_2+(C_3-a_1C_2)\exp\left(-\frac{C_3}{C_2}\tau\right)\right]\exp(-Ly),\end{aligned} \tag{29}$$

$$\begin{aligned}\Theta(y,\tau)=&\int_0^\infty \frac{\sqrt{a_0/\mathrm{Pr}_1}}{2\sqrt{\pi}u^{3/2}}\exp\left(\frac{-a_0/\mathrm{Pr}_1}{4u}-uy^2\right)\left[2\Phi(\tau)-1\right]du+\int_0^\infty\int_0^\tau\int_0^\pi \frac{1}{\pi}\frac{\sqrt{a_0/\mathrm{Pr}_1}}{2\sqrt{\pi}u^{3/2}}\frac{\sqrt{a_1uy^2}}{\sqrt{s}}\cos(\theta)\\
&\exp\left(\frac{-a_0/\mathrm{Pr}_1}{4u}-uy^2-a_1s+\left(2\sqrt{a_1uy^2s}\right)\cos(\theta)\right)d\theta dsdu,\end{aligned} \tag{30}$$

where, the Heaviside step function is represented by the notation $\Phi(\cdot)$. Note that neither Eq. (30) nor Eq. (31)'s final solutions contained any special functions. As the Caputo-Fabrizio fractional derivative lacks a unique kernel, this is the outcome of using it. The behaviour of fluids with

momentum and energy equations from Eq. (30) and (31) may be simply examined graphically with mathematical software such as Matlab and MathCad due to the lack of specific functions.

3.1 Skin Friction and Nusselt Number

By taking into account the following equations, the skin friction, $C_f(y,\tau)$ and Nusselt number, $Nu(y,\tau)$, for this particular problem are explored numerically and graphically [65,59]:

$$C_f(y,\tau) = -\beta_0(1-\phi_1)^{0.25}(1-\phi_2)^{0.25}\left.\frac{\partial \nu(y,\tau)}{\partial y}\right|_{y=0}, \tag{31}$$

and

$$Nu(y,\tau) = -\frac{k_{hnf}}{k_f}\left.\frac{\partial \Theta(y,\tau)}{\partial y}\right|_{y=0}. \tag{32}$$

The resulting Skin Friction and Nusselt Number solutions are explained in the following section.

4. Results and Discussion

In this section, the velocity and temperature profiles generated from Eq. (29) and (30) are generated *via* Mathcad15 and MATLAB. Thereafter, the profiles with distinctive values for each parameters are analysed. The base values for parameters are as follows:

$$\alpha = 0.2, \quad \gamma = 1, \quad E = 1, \quad Gr = 1, \quad \Pr = 6.2, \quad N = 1, \quad L = 5, \quad \phi = \phi_1 = \phi_2 = 0.01. \tag{33}$$

Since the impact of each nanoparticle on fluid flow is not the main focus of this study, the values of each type nanoparticles in the fluid will remain the same, which is 0.01 for both ϕ_1 and ϕ_2. Thus, the impact of nanoparticle volume fraction is summarised to the values of ϕ, instead of individually ϕ_1 and ϕ_2. Each parameter is used in every analysis and each analysis one parameter will have various values to analyse the impact of that parameter to the velocity and temperature of the fluid.

First, the velocity profile of the fluid with variations in the fractional parameter α is observed in Figure 3. It can be seen that the velocity of the fluid is increased when α is increased. The difference in speed showcases new solutions to the momentum equation when the fractional derivative is considered. Although the physical representation of fractional derivatives is still not known, obtained analytical solutions are pragmatic in future experimental and numerical studies.

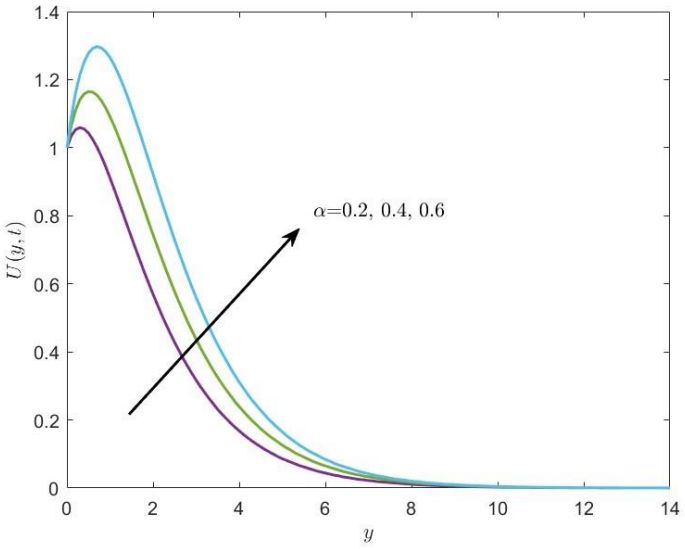

Fig. 3. Fluid velocity for distinctive values of α

Meanwhile, Figure 4 displays the velocity profile of the fluid with variations in the Casson parameter, γ. The Casson parameter determines the viscosity and plasticity of the fluid. A higher value of γ signifies a fluid with high viscosity and plasticity. High viscosity and plasticity of fluid would hinder fluid, slowing down the fluid. As observed in Figure 4, the velocity of the fluid decreases as the value of γ is increased.

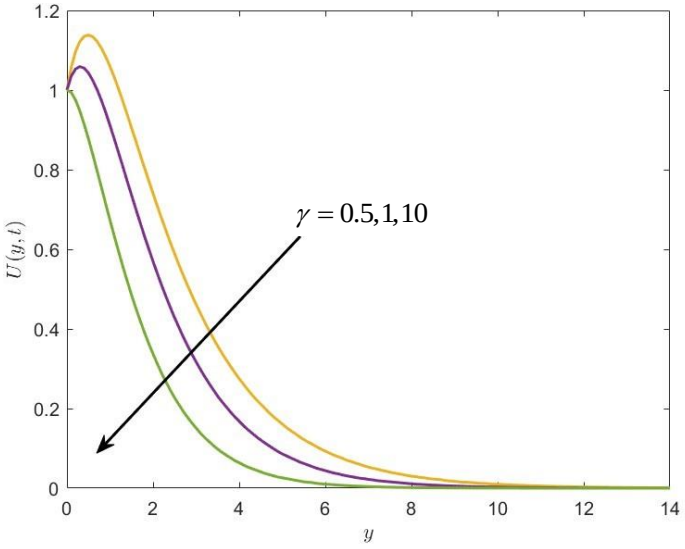

Fig. 4. Fluid velocity for distinctive values of γ

On the other hand, the fluid velocity increases with an increase in the modified Hartmann number, E. The presence of the Riga plate induces Lorentz force, and it is represented by the modified Hartmann number. As the E is increased, the Lorentz force is also increased, as observed in Figure 5. Since the position of the Riga plate induces Lorentz force in the direction of fluid flow, it causes the velocity of the fluid to increase. The increase in the velocity profile could also be due to the presence of Strontium Titanate ($SrTiO_3$) in the fluid. $SrTiO_3$ are excellent electrical conductors, aiding the fluid flow due to Lorentz force.

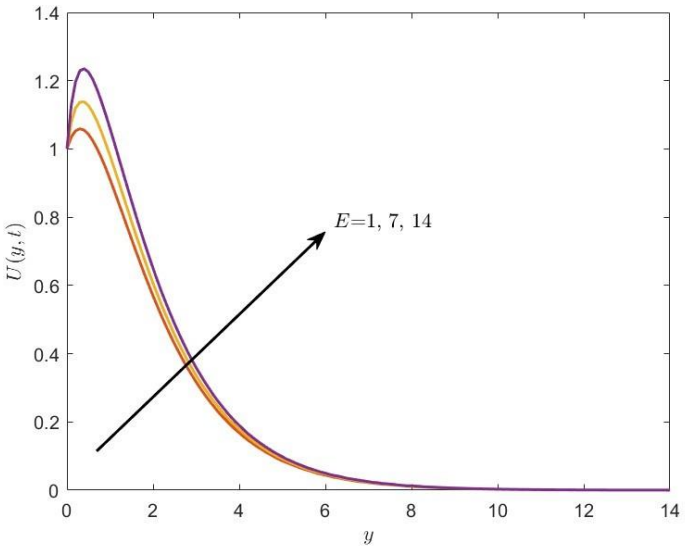

Fig. 5. Fluid velocity for distinctive values of E

Figure 6 observes the fluid velocity with various values of the Grashof number, Gr. Grashof number is defined as the correlation between the buoyancy force and the viscous force. When Gr is increased, the buoyancy force acting on the fluid is increased and in contrast, the viscous force of the fluid is increased. Thus, when the value of Gr is amplified, the velocity of the fluid is amplified as well, as observed in Figure 6.

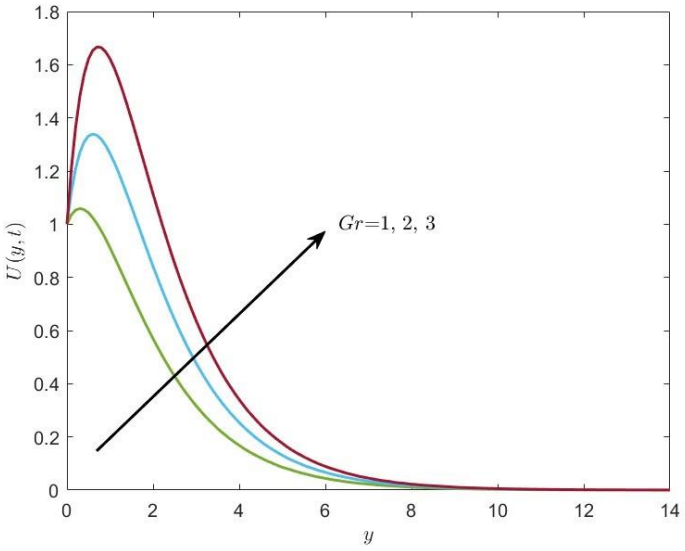

Fig. 6. Fluid velocity for distinctive values of Gr

The velocity of a fluid with different values of thermal radiation parameter, N, is showcased in Figure 7. An increase in N increases the magnitude of thermal radiation supplied to the fluid. Consequently raising the temperature of the fluid and increasing the kinetic energy within the fluid. Thus, increasing the fluid velocity. However, it is observed in Figure 7 that as the value of N is increased, the velocity of the fluid is decreased. This is due to the property of Strontium Titanate ($SrTiO_3$) considered in this study. Despite $SrTiO_3$ being excellent electrical conductors, they are very

poor in conducting heat. When exposed to extremely high temperatures, the functionality of $SrTiO_3$ is depleted, becoming excess weight within the fluid. Therefore, decreasing the velocity of the fluid.

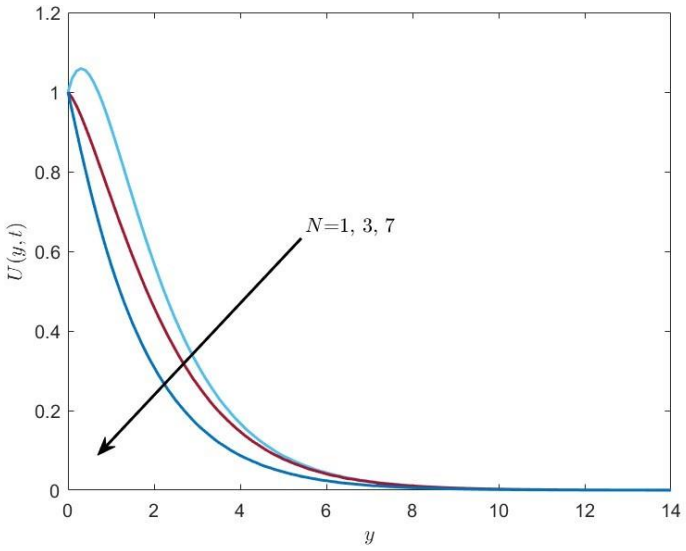

Fig. 7. Fluid velocity for distinctive values of N

Concurrently, the velocity profile for the fluid with various values of nanoparticle volume fraction, ϕ, is analysed from Figure 8. It is observed that as the value of ϕ is increased, fluid flow is slowed down. Although it is discussed that the presence of $SrTiO_3$ could aid in fluid flow, the overall volume of hybrid nanoparticles, including the Graphene nanoparticles, increases the mass of the fluid. As a result, the mass of the fluid countered the functionality of $SrTiO_3$ and decreases the fluid velocity.

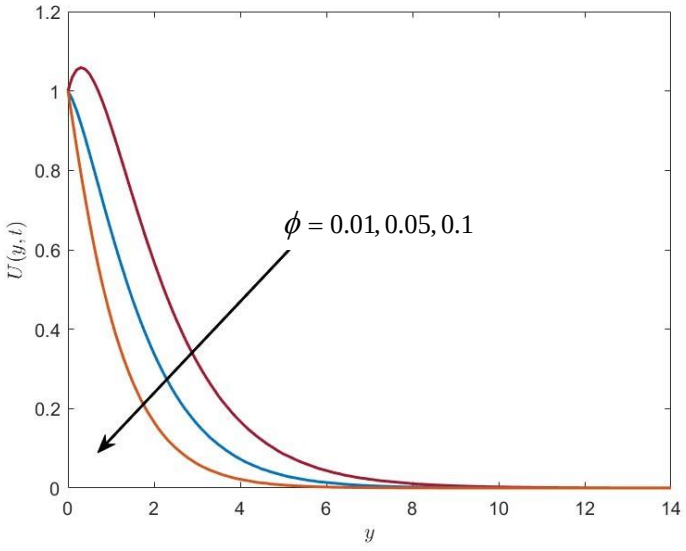

Fig. 8. Fluid velocity for distinctive values of ϕ

Meanwhile, Figure 9 shows the behaviour of the temperature of the fluid with increments in the fractional parameter, α. It is seen that the temperature of the fluid increase with every increment in the value of α. As discussed, fractional derivatives do not have a physical representation yet. However, these solutions will be useful in future experiments and numerical studies.

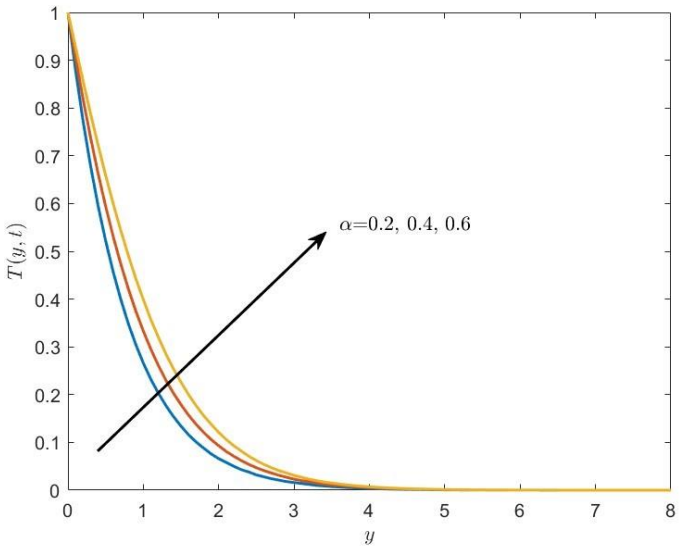

Fig. 9. Fluid temperature for distinctive values of α

Figure 10 on the other hand displays the temperature profile of the fluid with different values of the thermal radiation parameter, N. From the figure, it is seen that the fluid temperature increases with an increase in N. As the amount of N increases, the amount of thermal radiation supplied to fluid also increases. Thus, increasing the temperature of the fluid. It is also important to note that CMC fluid, the fluid considered in this study as the base fluid, has a very high specific heat capacity. Thus, a lot of energy is needed to increase the temperature of the fluid. Thus, it is also observed form Figure 10 that temperature of fluid is still high with large values of y.

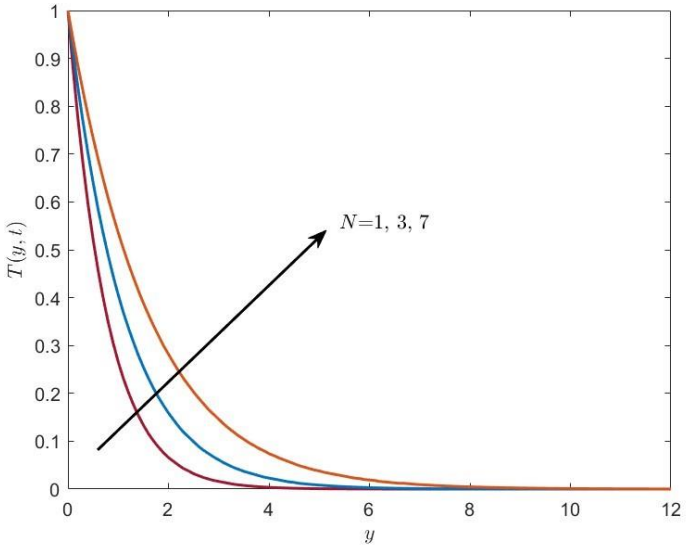

Fig. 10. Fluid temperature for distinctive values of N

The temperature of the fluid with several values of nanoparticle volume fraction, ϕ is elucidated in Figure 11. As values of ϕ increases, the amount of nanoparticles within the base fluid is increased. Since Graphene nanoparticles, part of the hybrid nanoparticle considered in this study, are excellent thermal conductors, the fluid temperature tends to increase with the increase of ϕ.

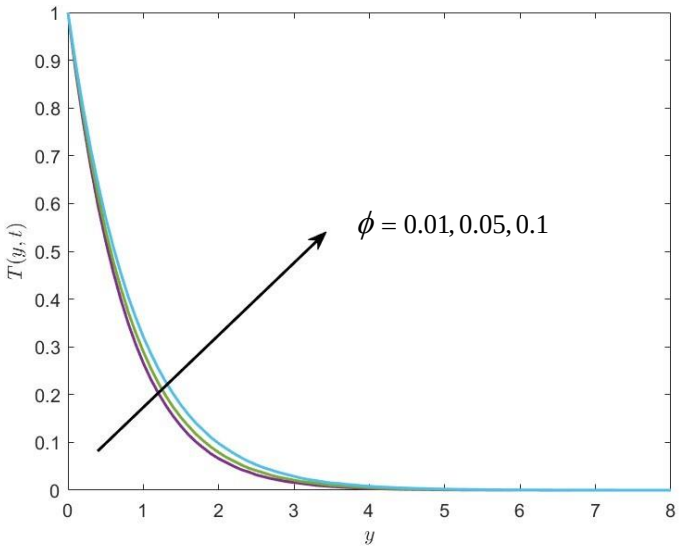

Fig. 11. Fluid temperature for distinctive values of ϕ

Skin friction, $C_f(y,\tau)$, analysis is displayed in Table 2. It is observed that $C_f(y,\tau)$ values correspond well to analysis on fluid velocity from Figures 3 to 8. The value of $C_f(y,\tau)$ when N is increased, skin friction is increased as well. As discussed, due to the properties of $SrTiO_3$, fluid velocity decreases. Thus, increasing the $C_f(y,\tau)$ value.

Table 2
Skin friction coefficients

α	γ	ϕ	E	Gr	N	$C_f(y,\tau)$
0.2	1	0.01	1	1	1	-0.837
0.6	1	0.01	1	1	1	-1.928
0.2	**5**	0.01	1	1	1	-0.095
0.2	1	**0.1**	1	1	1	0.819
0.2	1	0.01	**3**	1	1	-1.195
0.2	1	0.01	1	**2**	1	-2.632
0.2	1	0.01	1	1	**3**	0.216

On the other hand, the Nusselt number, $Nu(y,\tau)$, for fluid flow is analysed in Table 3. Values of $Nu(y,\tau)$ correspond to the analysis of fluid temperature from Figures 9 to 11. It is important to note that since CMC is considered as the base fluid in this study, the heat transfer rate is reduced. This is due to the very high specific capacity of CMC fluid.

Table 3
Nusselt numbers

α	ϕ	N	$Nu(y,\tau)$
0.2	0.01	1	1.350
0.6	0.01	1	0.771
0.2	**0.1**	1	1.858
0.2	0.01	**3**	0.928

5. Conclusions

An analytical study on fractional Caputo-Fabrizio Mxene Strontium Titanate Hybrid Nanofluid with Carboxymethyl Cellulose base flowing over a vertical uniform velocity Riga plate has been done. Final solutions in integral form with fractional parameters α were obtained via Laplace transform and analysed graphically and numerically. It is observed that:

i. Fluid velocity and temperature increase with an increase in fractional parameter α.
ii. Fluid velocity decreases with an increase in thermal radiation, N. In contrast, the fluid temperature increases.
iii. Fluid velocity decreases with an increase in nanoparticle volume fraction, ϕ. In contrast, the fluid temperature increases.
iv. Fluid velocity decreases with an increase in Casson parameter, γ.
v. Fluid velocity increases with an increase in the modified Hartmann number, E.
vi. Fluid temperature increases with an increase in Grashof number, Gr.
vii. Skin friction and Nusselt number correspond well with graphical analyses.

Acknowledgement
This research was funded by Universiti Teknologi Malaysia under Matching Grant Scheme R.J130000.7354.4B748 and Q.J130000.3054.03M77.

References
[1] Choi, S. US, and Jeffrey A. Eastman. *Enhancing thermal conductivity of fluids with nanoparticles*. No. ANL/MSD/CP-84938; CONF-951135-29. Argonne National Lab.(ANL), Argonne, IL (United States), 1995.
[2] Khalid, Asma, Ilyas Khan, and Sharidan Shafie. "Exact solutions for free convection flow of nanofluids with ramped wall temperature." *The European Physical Journal Plus* 130 (2015): 1-14. https://doi.org/10.1140/epjp/i2015-15057-9
[3] Aly, Emad H., and Abdelhalim Ebaid. "Exact analysis for the effect of heat transfer on MHD and radiation Marangoni boundary layer nanofluid flow past a surface embedded in a porous medium." *Journal of Molecular liquids* 215 (2016): 625-639. https://doi.org/10.1016/j.molliq.2015.12.108
[4] Prasad, P. Durga, RVMSS Kiran Kumar, and S. V. K. Varma. "Heat and mass transfer analysis for the MHD flow of nanofluid with radiation absorption." *Ain Shams Engineering Journal* 9, no. 4 (2018): 801-813. https://doi.org/10.1016/j.asej.2016.04.016
[5] Hussanan, Abid, Mohd Zuki Salleh, Ilyas Khan, and Zhi-Min Chen. "Unsteady water functionalized oxide and non-oxide nanofluids flow over an infinite accelerated plate." *Chinese Journal of Physics* 62 (2019): 115-131. https://doi.org/10.1016/j.cjph.2019.09.020
[6] Souayeh, Basma, M. Gnaneswara Reddy, P. Sreenivasulu, T. M. I. M. Poornima, Mohammad Rahimi-Gorji, and Ibrahim M. Alarifi. "Comparative analysis on non-linear radiative heat transfer on MHD Casson nanofluid past a thin needle." *Journal of Molecular Liquids* 284 (2019): 163-174. https://doi.org/10.1016/j.molliq.2019.03.151

[7] Uddin, M. J., and S. K. Rasel. "Numerical analysis of natural convective heat transport of copper oxide-water nanofluid flow inside a quadrilateral vessel." *Heliyon* 5, no. 5 (2019). https://doi.org/10.1016/j.heliyon.2019.e01757
[8] Mahanta, G., M. Das, S. Shaw, and K. L. Mahanta. "Heat and mass transfer of Casson nanofluid flow over a stretching sheet in the presence of magnetic field with Brownian and thermophoretic effects." *Journal of Engineering Science & Technology* 14, no. 5 (2019): 3046-3061.
[9] Krishna, M. Veera, and Ali J. Chamkha. "Hall and ion slip effects on MHD rotating boundary layer flow of nanofluid past an infinite vertical plate embedded in a porous medium." *Results in Physics* 15 (2019): 102652. https://doi.org/10.1016/j.rinp.2019.102652
[10] Aleem, Maryam, Muhammad Imran Asjad, Aqila Shaheen, and Ilyas Khan. "MHD Influence on different water based nanofluids (TiO2, Al2O3, CuO) in porous medium with chemical reaction and newtonian heating." *Chaos, Solitons & Fractals* 130 (2020): 109437. https://doi.org/10.1016/j.chaos.2019.109437
[11] Anwar, Talha, Poom Kumam, and Wiboonsak Watthayu. "An exact analysis of unsteady MHD free convection flow of some nanofluids with ramped wall velocity and ramped wall temperature accounting heat radiation and injection/consumption." *Scientific Reports* 10, no. 1 (2020): 17830. https://doi.org/10.1038/s41598-020-74739-w
[12] VahidMohammadi, Armin, Johanna Rosen, and Yury Gogotsi. "The world of two-dimensional carbides and nitrides (MXenes)." *Science* 372, no. 6547 (2021): eabf1581. https://doi.org/10.1126/science.abf1581
[13] Wu, Zhitan, Tongxin Shang, Yaqian Deng, Ying Tao, and Quan-Hong Yang. "The assembly of MXenes from 2D to 3D." *Advanced Science* 7, no. 7 (2020): 1903077. https://doi.org/10.1002/advs.201903077
[14] Baig, Mutawara Mahmood, Iftikhar Hussain Gul, Sherjeel Mahmood Baig, and Faisal Shahzad. "2D MXenes: synthesis, properties, and electrochemical energy storage for supercapacitors–a review." *Journal of Electroanalytical Chemistry* 904 (2022): 115920. https://doi.org/10.1016/j.jelechem.2021.115920
[15] Zhu, Jing, Enna Ha, Guoliang Zhao, Yang Zhou, Deshun Huang, Guozong Yue, Liangsheng Hu et al. "Recent advance in MXenes: a promising 2D material for catalysis, sensor and chemical adsorption." *Coordination Chemistry Reviews* 352 (2017): 306-327. https://doi.org/10.1016/j.ccr.2017.09.012
[16] Zhang, Yi-Zhou, Jehad K. El-Demellawi, Qiu Jiang, Gang Ge, Hanfeng Liang, Kanghyuck Lee, Xiaochen Dong, and Husam N. Alshareef. "MXene hydrogels: fundamentals and applications." *Chemical Society Reviews* 49, no. 20 (2020): 7229-7251. https://doi.org/10.1039/D0CS00022A
[17] Rehman, Jalil Ur, M. Awais Rehman, M. Bilal Tahir, Abid Hussain, Tahir Iqbal, Muhammad Sagir, Muhammad Usman, Imen Kebaili, Hussein Alrobei, and Meshal Alzaid. "Electronic and optical properties of nitrogen and sulfur doped strontium titanate as efficient photocatalyst for water splitting: a DFT study." *International Journal of Hydrogen Energy* 47, no. 3 (2022): 1605-1612. https://doi.org/10.1016/j.ijhydene.2021.10.133
[18] Duan, Yuhua, Paul Ohodnicki, Benjamin Chorpening, and Gregory Hackett. "Electronic structural, optical and phonon lattice dynamical properties of pure-and La-doped SrTiO3: An ab initio thermodynamics study." *Journal of Solid State Chemistry* 256 (2017): 239-251. https://doi.org/10.1016/j.jssc.2017.09.016
[19] Xu, Qiang, Shuyan Ye, Weizhi Liu, Yanshuang Chen, Qiyu Chen, and Liejin Guo. "Intelligent identification of steam jet condensation regime in water pipe flow system by wavelet multiresolution analysis of pressure oscillation and artificial neural network." *Applied Thermal Engineering* 147 (2019): 1047-1058. https://doi.org/10.1016/j.applthermaleng.2018.11.005
[20] Sarkar, Jahar, Pradyumna Ghosh, and Arjumand Adil. "A review on hybrid nanofluids: recent research, development and applications." *Renewable and Sustainable Energy Reviews* 43 (2015): 164-177. https://doi.org/10.1016/j.rser.2014.11.023
[21] Sidik, Nor Azwadi Che, Isa Muhammad Adamu, Muhammad Mahmud Jamil, G. H. R. Kefayati, Rizalman Mamat, and G. Najafi. "Recent progress on hybrid nanofluids in heat transfer applications: a comprehensive review." *International communications in heat and mass Transfer* 78 (2016): 68-79. https://doi.org/10.1016/j.icheatmasstransfer.2016.08.019
[22] Xian, Hong Wei, Nor Azwadi Che Sidik, Siti Rahmah Aid, Tan Lit Ken, and Yutaka Asako. "Review on Preparation Techniques, Properties and Performance of Hybrid Nanofluid in Recent Engineering Application." *Journal of Advanced Research in Fluid Mechanics and Thermal Sciences* 45, no. 1 (2018): 1-13.
[23] Sajid, Muhammad Usman, and Hafiz Muhammad Ali. "Thermal conductivity of hybrid nanofluids: a critical review." *International Journal of Heat and Mass Transfer* 126 (2018): 211-234. https://doi.org/10.1016/j.ijheatmasstransfer.2018.05.021
[24] Muneeshwaran, M., G. Srinivasan, P. Muthukumar, and Chi-Chuan Wang. "Role of hybrid-nanofluid in heat transfer enhancement–A review." *International Communications in Heat and Mass Transfer* 125 (2021): 105341. https://doi.org/10.1016/j.icheatmasstransfer.2021.105341

[25] Rahman, Md Saifur, Md Saif Hasan, Ashis Sutradhar Nitai, Sunghyun Nam, Aneek Krishna Karmakar, Md Shameem Ahsan, Muhammad JA Shiddiky, and Mohammad Boshir Ahmed. "Recent developments of carboxymethyl cellulose." *Polymers* 13, no. 8 (2021): 1345. https://doi.org/10.3390/polym13081345

[26] Radi, Mohsen, and Sedigheh Amiri. "Comparison of the rheological behavior of solutions and formulated oil-in-water emulsions containing carboxymethylcellulose (CMC)." *Journal of dispersion science and technology* 34, no. 4 (2013): 582-589. https://doi.org/10.1080/01932691.2012.681607

[27] Lee, Hyundo, and Byoungseung Yoo. "Rheological characteristics of waxy rice starch modified by carboxymethyl cellulose." *Preventive Nutrition and Food Science* 24, no. 4 (2019): 478. https://doi.org/10.3746/pnf.2019.24.4.478

[28] Alwawi, Firas A., Hamzeh T. Alkasasbeh, Ahmed M. Rashad, and Ruwaidiah Idris. "A numerical approach for the heat transfer flow of carboxymethyl cellulose-water based Casson nanofluid from a solid sphere generated by mixed convection under the influence of Lorentz force." *Mathematics* 8, no. 7 (2020): 1094. https://doi.org/10.3390/math8071094

[29] Ali, Farhan, T. Arun Kumar, K. Loganathan, C. S. Reddy, Amjad Ali Pasha, Mustafa Mutiur Rahman, and Khaled Al-Farhany. "Irreversibility analysis of cross fluid past a stretchable vertical sheet with mixture of Carboxymethyl cellulose water based hybrid nanofluid." *Alexandria Engineering Journal* 64 (2023): 107-118. https://doi.org/10.1016/j.aej.2022.08.037

[30] Rawi, N. A., M. R. Ilias, Y. J. Lim, Z. M. Isa, and S. Shafie. "Unsteady mixed convection flow of Casson fluid past an inclined stretching sheet in the presence of nanoparticles." In *Journal of Physics: Conference Series*, vol. 890, no. 1, p. 012048. IOP Publishing, 2017. https://doi.org/10.1088/1742-6596/890/1/012048

[31] Saqib, Muhammad, Ilyas Khan, and Sharidan Shafie. "Application of Atangana–Baleanu fractional derivative to MHD channel flow of CMC-based-CNT's nanofluid through a porous medium." *Chaos, Solitons & Fractals* 116 (2018): 79-85. https://doi.org/10.1016/j.chaos.2018.09.007

[32] Saqib, Muhammad, Ilyas Khan, and Sheridan Shafie. "Natural convection channel flow of CMC-based CNTs nanofluid." *The European Physical Journal Plus* 133, no. 12 (2018): 549. https://doi.org/10.1140/epjp/i2018-12340-3

[33] Luchko, Yuri. "Fractional derivatives and the fundamental theorem of fractional calculus." *Fractional Calculus and Applied Analysis* 23, no. 4 (2020): 939-966. https://doi.org/10.1515/fca-2020-0049

[34] Atangana, Abdon, and Dumitru Baleanu. "Numerical solution of a kind of fractional parabolic equations via two difference schemes." In *Abstract and Applied Analysis*, vol. 2013. Hindawi, 2013. https://doi.org/10.1155/2013/828764

[35] Teodoro, G. Sales, JA Tenreiro Machado, and E. Capelas De Oliveira. "A review of definitions of fractional derivatives and other operators." *Journal of Computational Physics* 388 (2019): 195-208. https://doi.org/10.1016/j.jcp.2019.03.008

[36] Khan, Ilyas, Nehad Ali Shah, and Dumitru Vieru. "Unsteady flow of generalized Casson fluid with fractional derivative due to an infinite plate." *The European physical journal plus* 131 (2016): 1-12. https://doi.org/10.1140/epjp/i2016-16181-8

[37] Abro, K. A., and I. Khan. "Effects of CNTs on magnetohydrodynamic flow of methanol based nanofluids via Atangana-Baleanu and Caputo-Fabrizio fractional derivatives. vol. 1." *Therm Sci* (2018): 1-12.

[38] Maiti, S., S. Shaw, and G. C. Shit. "Caputo–Fabrizio fractional order model on MHD blood flow with heat and mass transfer through a porous vessel in the presence of thermal radiation." *Physica A: Statistical Mechanics and its Applications* 540 (2020): 123149. https://doi.org/10.1016/j.physa.2019.123149

[39] Raza, Nauman, and Muhammad Asad Ullah. "A comparative study of heat transfer analysis of fractional Maxwell fluid by using Caputo and Caputo–Fabrizio derivatives." *Canadian Journal of Physics* 98, no. 1 (2020): 89-101. https://doi.org/10.1139/cjp-2018-0602

[40] Reyaz, Ridhwan, Ahmad Qushairi Mohamad, Yeou Jiann Lim, Muhammad Saqib, and Sharidan Shafie. "Analytical solution for impact of Caputo-Fabrizio fractional derivative on MHD casson fluid with thermal radiation and chemical reaction effects." *Fractal and Fractional* 6, no. 1 (2022): 38. https://doi.org/10.3390/fractalfract6010038

[41] Sene, Ndolane. "Analytical solutions of a class of fluids models with the Caputo fractional derivative." *Fractal and Fractional* 6, no. 1 (2022): 35. https://doi.org/10.3390/fractalfract6010035

[42] Reyaz, Ridhwan, Ahmad Qushairi Mohamad, Lim Yeou Jiann, Muhammad Saqib, and Sharidan Shafie. "Presence of Riga plate on MHD Caputo Casson fluid: an analytical study." *Journal of Advanced Research in Fluid Mechanics and Thermal Sciences* 93, no. 2 (2022): 86-99. https://doi.org/10.37934/arfmts.93.2.8699

[43] Asogwa, Kanayo K., M. D. Alsulami, B. C. Prasannakumara, and Taseer Muhammad. "Double diffusive convection and cross diffusion effects on Casson fluid over a Lorentz force driven Riga plate in a porous medium with heat sink: An analytical approach." *International Communications in Heat and Mass Transfer* 131 (2022): 105761. https://doi.org/10.1016/j.icheatmasstransfer.2021.105761

[44] Asogwa, Kanayo K., F. Mebarek-Oudina, and I. L. Animasaun. "Comparative investigation of water-based Al2O3 nanoparticles through water-based CuO nanoparticles over an exponentially accelerated radiative Riga plate surface via heat transport." *Arabian Journal for Science and Engineering* 47, no. 7 (2022): 8721-8738. https://doi.org/10.1007/s13369-021-06355-3

[45] Khatun, Sheela, Muhammad Minarul Islam, Md Tusher Mollah, Saykat Poddar, and Md Mahmud Alam. "EMHD radiating fluid flow along a vertical Riga plate with suction in a rotating system." *SN Applied Sciences* 3 (2021): 1-14. https://doi.org/10.1007/s42452-021-04444-4

[46] Mallawi, F. O. M., M. Bhuvaneswari, S. Sivasankaran, and S. Eswaramoorthi. "Impact of double-stratification on convective flow of a non-Newtonian liquid in a Riga plate with Cattaneo-Christov double-flux and thermal radiation." *Ain Shams Engineering Journal* 12, no. 1 (2021): 969-981. https://doi.org/10.1016/j.asej.2020.04.010

[47] Rasool, Ghulam, Anum Shafiq, and Chaudry Masood Khalique. "Marangoni forced convective Casson type nanofluid flow in the presence of Lorentz force generated by Riga plate." *Discrete & Continuous Dynamical Systems-Series S* 14, no. 7 (2021). https://doi.org/10.3934/dcdss.2021059

[48] Bilal, S., Kanayo K. Asogwa, Hammad Alotaibi, M. Y. Malik, and Ilyas Khan. "Analytical treatment of radiative Casson fluid over an isothermal inclined Riga surface with aspects of chemically reactive species." *Alexandria Engineering Journal* 60, no. 5 (2021): 4243-4253. https://doi.org/10.1016/j.aej.2021.03.015

[49] Loganathan, Parasuraman, and M. Dhivya. "Heat and mass transfer analysis of a convective Williamson fluid flow over a cylinder." *International Journal of Fluid Mechanics Research* 47, no. 2 (2020). https://doi.org/10.1615/InterJFluidMechRes.2020027371

[50] Nasrin, Sonia, Rabindra Nath Mondal, and Md Mahmud Alam. "Impulsively started horizontal Riga plate embedded in unsteady Casson fluid flow with rotation." *Journal of Applied Mathematics and Physics* 8, no. 9 (2020): 1861-1876. https://doi.org/10.4236/jamp.2020.89140

[51] Asogwa, Kanayo K., Sardar M. Bilal, Isaac L. Animasaun, and Fateh M. Mebarek-Oudina. "Insight into the significance of ramped wall temperature and ramped surface concentration: The case of Casson fluid flow on an inclined Riga plate with heat absorption and chemical reaction." *Nonlinear Engineering* 10, no. 1 (2021): 213-230. https://doi.org/10.1515/nleng-2021-0016

[52] Shahrim, Muhammad Nazirul, Ahmad Qushairi Mohamad, Lim Yeou Jiann, Muhamad Najib Zakaria, Sharidan Shafie, Zulkhibri Ismail, and Abdul Rahman Mohd Kasim. "Exact solution of fractional convective Casson fluid through an accelerated plate." *CFD Letters* 13, no. 6 (2021): 15-25. https://doi.org/10.37934/cfdl.13.6.1525

[53] Hussanan, Abid, Mohd Zuki Salleh, Ilyas Khan, and Razman Mat Tahar. "Heat transfer in magnetohydrodynamic flow of a Casson fluid with porous medium and Newtonian heating." *Journal of nanofluids* 6, no. 4 (2017): 784-793. https://doi.org/10.1166/jon.2017.1359

[54] Zakaria, Muhamad Najib, Abid Hussanan, Ilyas Khan, and Sharidan Shafie. "The effects of radiation on free convection flow with ramped wall temperature in Brinkman type fluid." *Jurnal Teknologi* 62, no. 3 (2013): 33-39. https://doi.org/10.11113/jt.v62.1886

[55] Anantha Kumar, K., V. Sugunamma, and N. Sandeep. "Effect of thermal radiation on MHD Casson fluid flow over an exponentially stretching curved sheet." *Journal of Thermal Analysis and Calorimetry* 140 (2020): 2377-2385. https://doi.org/10.1007/s10973-019-08977-0

[56] Yusof, Nur Syamila, Siti Khuzaimah Soid, Mohd Rijal Illias, Ahmad Sukri Abd Aziz, and Nor Ain Azeany Mohd Nasir. "Radiative Boundary Layer Flow of Casson Fluid Over an Exponentially Permeable Slippery Riga Plate with Viscous Dissipation." *Journal of Advanced Research in Applied Sciences and Engineering Technology* 21, no. 1 (2020): 41-51. https://doi.org/10.37934/araset.21.1.4151

[57] Waini, Iskandar, Anuar Ishak, and Ioan Pop. "Symmetrical solutions of hybrid nanofluid stagnation-point flow in a porous medium." *International Communications in Heat and Mass Transfer* 130 (2022): 105804. https://doi.org/10.1016/j.icheatmasstransfer.2021.105804

[58] Hosseinzadeh, Kh, A. Asadi, A. R. Mogharrebi, M. Ermia Azari, and D. D. Ganji. "Investigation of mixture fluid suspended by hybrid nanoparticles over vertical cylinder by considering shape factor effect." *Journal of Thermal Analysis and Calorimetry* 143, no. 2 (2021): 1081-1095. https://doi.org/10.1007/s10973-020-09347-x

[59] Krishna, M. Veera, N. Ameer Ahammad, and Ali J. Chamkha. "Radiative MHD flow of Casson hybrid nanofluid over an infinite exponentially accelerated vertical porous surface." *Case Studies in Thermal Engineering* 27 (2021): 101229. https://doi.org/10.1016/j.csite.2021.101229

[60] Khan, M., S. Hyder Ali, and Haitao Qi. "Some accelerated flows for a generalized Oldroyd-B fluid." *Nonlinear analysis: real world applications* 10, no. 2 (2009): 980-991. https://doi.org/10.1016/j.nonrwa.2007.11.017

[61] Khan, M., S. Hyder Ali, and C. Fetecau. "Exact solutions of accelerated flows for a Burgers' fluid II. The cases γ= λ 2/4 and γ> λ 2/4." *Zeitschrift für angewandte Mathematik und Physik* 60 (2009): 701-722. https://doi.org/10.1007/s00033-008-7155-6

[62] Hussanan, Abid, Mohd Zuki Salleh, Ilyas Khan, and Razman Mat Tahar. "Unsteady heat transfer flow of a Casson fluid with Newtonian heating and thermal radiation." *Jurnal Teknologi* 78, no. 4 (2016): 1-7. https://doi.org/10.11113/jt.v78.8264

[63] Mohamad, Ahmad Qushairi, Ilyas Khan, Lim Yeou Jiann, Sharidan Shafie, Zaiton Mat Isa, and Zulkhibri Ismail. "Heat transfer on rotating second grade fluid through an accelerated plate." *Malaysian Journal of Fundamental and Applied Sciences* 13, no. 3 (2017): 219-223. https://doi.org/10.11113/mjfas.v13n3.645

[64] Hussanan, Abid, Mohd Zuki Salleh, Razman Mat Tahar, and Ilyas Khan. "Unsteady boundary layer flow and heat transfer of a Casson fluid past an oscillating vertical plate with Newtonian heating." *PloS one* 9, no. 10 (2014): e108763. https://doi.org/10.1371/journal.pone.0108763

[65] Ali, Farhad, Muhammad Arif, Ilyas Khan, Nadeem A. Sheikh, and Muhammad Saqib. "Natural convection in polyethylene glycol based molybdenum disulfide nanofluid with thermal radiation, chemical reaction and ramped wall temperature." *International Journal of Heat and Technology* (2018). https://doi.org/10.18280/ijht.360227